



Measurement of radionuclide contents and $^{222}\text{Rn}/^{220}\text{Rn}$ exhalation rate in soil samples from sub-mountainous region of India

Manpreet Kaur^{1,2} · Ajay Kumar¹ · Rohit Mehra² · Rosaline Mishra³ · Bikramjit Singh Bajwa⁴

Received: 19 August 2019 / Accepted: 12 April 2021 / Published online: 2 May 2021
© Saudi Society for Geosciences 2021

Abstract

The present study involves the measurement of radionuclide contents and radon/thoron exhalation rate in the soil samples collected from the 30 villages of Jammu district, J & K, India. Thallium-doped sodium iodide detector and advanced Smart Rn Duo monitor were used for the measurement of the radionuclide contents and radon/thoron exhalation rates. The radon flux rate was also measured by using a surface chamber technique. The radon mass exhalation rate in the soil samples has been found to vary from 15 ± 0.4 to 38 ± 0.8 $\text{mBq kg}^{-1} \text{h}^{-1}$, while thoron surface exhalation rate has been found to vary from 90 ± 22 to 4880 ± 280 $\text{Bq m}^{-2} \text{h}^{-1}$. The mean value of radium equivalent activity (99 ± 27 Bq kg^{-1}) has appeared to be well within the admissible limit of 370 Bq kg^{-1} suggested by the Organization for Economic Cooperation and Development (2009) report. The values of various parameters related to radiological hazards were also calculated, and all parameters have been found to be well below the safe limits given by various organizations. The outcomes pointed out that the region was protected from danger as per health risk effects associated with these radionuclide contents are concerned.

Keywords Absorbed dose rate · Exhalation rate · Human health · Radionuclide · Smart Rn Duo monitor

Introduction

The process of emission of radon and thoron from the soil and other materials by the radioactive decay of radium and thorium is considered as the most important parameters for evaluating the behavior and concentrations of environmental ^{222}Rn and ^{220}Rn . Their exhalation rate depends upon many physical factors associated with soil as soil morphology, soil mineralogy, size of soil grain, soil porosity, and soil permeability. It also depends upon some other parameters such as radium and

thorium content in the soil and emanation coefficient of soil grains (Aburnurad and Al-Tamimi 2001). The more porous the material, the higher the chance of radon exhalation from soil because of eminent diffusion of the radon gas. Radon can exhale from the orifice volume into the environment assignable to diffusion and convection. The high indoor radon concentration from soil because of their elevated radon exhalation rates can be assigned to strong uranium/radium enrichment. Therefore, it is significant to quantify the level of radon and thoron exhalation rate from the soil. This information is helpful in locating zones with a danger of high radon and thoron exposure.

The main contribution to the radioactivity of the soil comes from the decay series of the primordial radionuclides ^{238}U and ^{232}Th and other specific radionuclide ^{40}K . The gamma-ray emissions from radionuclide and α particles emitted during the decay of ^{238}U , ^{226}Ra , ^{222}Rn , ^{220}Rn , and their progeny possess exposure risk to human beings (UNSCEAR 2000a). According to the National Council on Radiation Protection and Measurements (1987), about 82% of the radiation dose taken by humans are because of natural radiation sources, while the rest is due to anthropogenic reasons. The natural radionuclide concentration in environmental samples varies with the geographical and geological features of the region.

Responsible Editor: Amjad Kallel

✉ Ajay Kumar
ajay782@rediffmail.com

¹ Department of Physics, DAV College, Amritsar, Punjab 143001, India

² Department of Physics, Dr. B. R. Ambedkar National Institute of Technology, Jalandhar, Punjab 144001, India

³ Radiological Physics & Advisory Division, Bhabha Atomic Research Centre, Mumbai, Maharashtra 400085, India

⁴ Department of Physics, Guru Nanak Dev University, Amritsar, Punjab 143005, India

The knowledge regarding these natural radionuclides content levels and their impact on the environment is of great significance in various fields like science and engineering (IAEA 2002; Jadiyahpa 2018).

Many researchers worldwide are engaged in the field of natural radioactivity measurements (Al-Jundia et al. 2003; Agbalagba and Onoja 2011; Kumar et al. 2009; Mir and Rather 2015) and measurements of the soil exhalation rate of radon and thoron (Ielsch et al. 2002; Rafique et al. 2011; Saad et al. 2013; Sun et al. 2004) which has resulted in worldwide mapping to assess the impact of exposure to human health due to its carcinogenic nature.

As per the latest literature survey in the northern part of India, measurements of natural radioactivity and radon/thoron exhalation rates have been carried out in some areas of Punjab (Badhan and Mehra 2012; Mehta et al. 2015) and Himachal Pradesh (Sharma et al. 2003; Singh et al. 2016). But no research study was conducted previously for the assessment of radon/thoron exhalation rates and radionuclide contents in soil samples of Jammu district, J & K. Therefore, this work aims at the determination of the natural radioactivity and radon/thoron exhalation rates in soil samples with known characteristics (porosity, density, and emanation factor and radon flux rate) to keep reference records for future investigation and mapping. The potential radiological hazards associated with the studied materials were also assessed and compared with the values published by various agencies. The main purpose of the present work is to determine the levels of natural radioactivity, to calculate exhalation rates, and to look out for health-related risks to the inhabitants of the area under study.

Geology of the study area

Figure 1 illustrates the survey zone of Jammu district, which is a part of northern India and is the southernmost region of J & K state. Geographically, it expands from latitudes $32^{\circ} 33' 07''$ to $33^{\circ} 07' 30''$ north and longitudes $73^{\circ} 51' 19''$ to $75^{\circ} 08' 52''$ east. Jammu lies in the sub-mountain region, in the foothills of the Himalayas. The sediments of outer plains have been laid down by the descending rivers, debouching the plains and shaded their sediment load. These sediments contain gravels, pebbles, sand, boulders, and clays. These outer plains are categorized into the “Kandi” channel along the north in which the characteristics of rocks differ from clusters of clay, including stone, and the other “Sirowal” channel along the south which includes only supreme alluvium such as sludge.

Physiographically speaking, the zone involves two utmost sections stretching all over the district. One section is the mountainous belt of Siwalik formations which spreads in the northern segment, whereas the other section is a plain belt, comprising the southern segment (Kaur et al. 2018a). The plain belt fuses with the Indogangetic plain along the south,

and the Siwalik range ascends step by step along north of the zone. The Siwalik range spreads between the Himalayan Frontal Thrust (HFT) in the southern part and the Main Boundary Thrust (MBT) in the northern part and splits in lower, middle, and upper Siwalik emergences. Lithostratigraphic units of the Siwalik formations are summarized as follows:

The rocks of lower Siwalik have a wide range of sedimentary rocks from a dark red consolidated mud to yellow sand or quartz grains which are cemented together, and their progression involves basically moderate clay. The sand is less dense with variation in their size from fine to average. However, the rocks of the middle Siwalik range between upper Miocene and lower Pliocene, and they are mostly sandy formed from grayish and brownish mud. The sandstones vary in size from large to medium grained and are delicate.

The upper Siwalik subgroup ranges in age from upper Pliocene to Pleistocene age. The upper Siwalik subgroup has two faces. The lower part is sandy with conglomerate intercalations, whereas in the upper part, cobble and boulder conglomerates are dominant. The sandstones of the lower part are medium to coarse grained, soft, pebbly and gray in color and alternate with conglomerates having a pebble casts. Overlying these faces are the thick cobble and boulder conglomerate beds.

There are two categories of soils, i.e., lithosols and alluvial soil. Lithosols are observed on sheer slants in the foothills of the region, and the soil diversifies from parched to slime fertile clay along pebbles in a minute ratio. Alluvial soil substantially appears along the outer plain area which is fertile with a small proportion of clay and contains a little amount of lime with good magnesium quantity.

Experimental technique

Sampling

In the present study, the soil samples from 30 villages of Jammu district were assembled 30 cm deep inside the soil's surface to get natural, static, and pure samples that have not been mixed up with environmental impurities. Only one soil sample of mass about 1000g was taken from each village, and assembled samples were placed in polyethylene sealable flaps, named properly, and studied at the DAV College, Nuclear Research Lab, for further analysis. These samples were left in the open air (Kaur et al. 2018b) before exhalation measurement. Figure 2 represents the flow chart of the research methodology for the present work.

Statistical analysis

The normality of the data was checked by the Shapiro-Wilk test (Shapiro and Wilk 1965). The Mann-Whitney non-

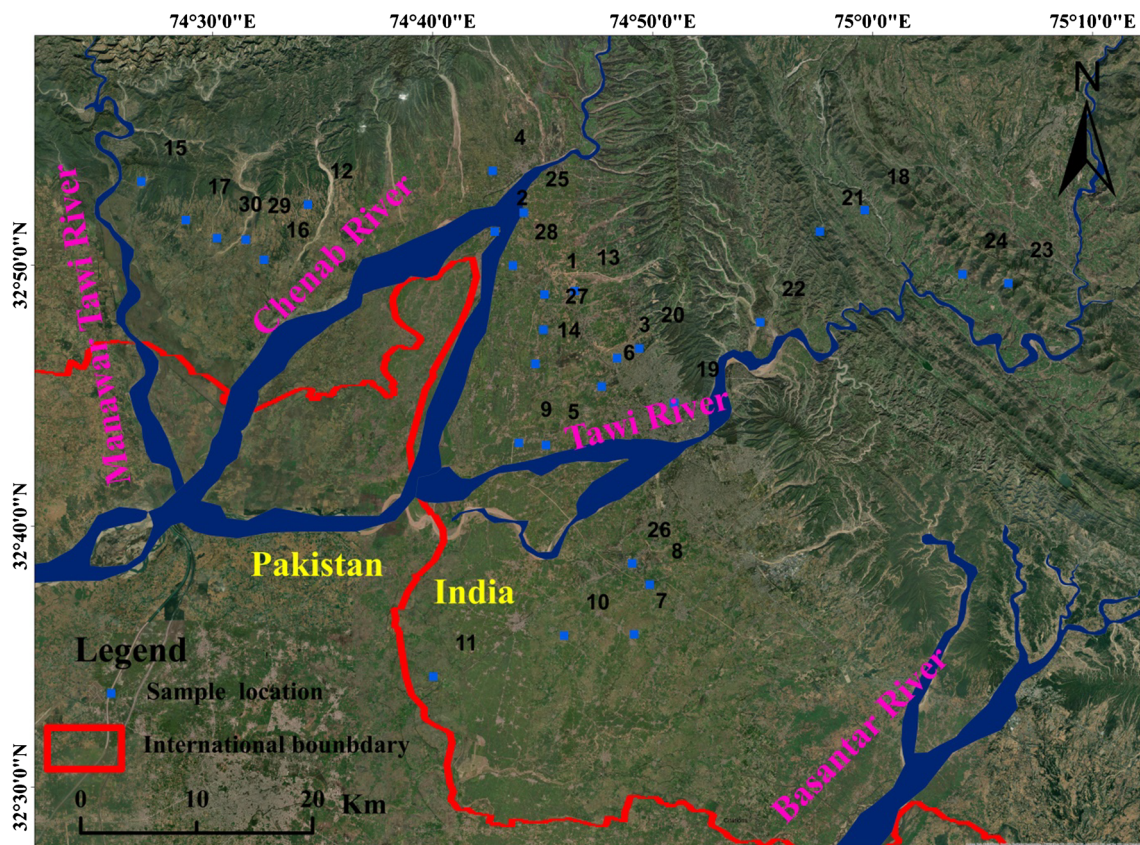


Fig. 1 Geological map of surveyed locations of Jammu district, Jammu and Kashmir, India

parametric homogeneity test (Mann and Whitney 1947) studied the contrast of medians to detect uniformity. Marked dissimilarity within the contents of the radon flux rate was observed for in situ and empirical methods. Every statistical task was done at a standard significant level (0.05).

Exhalation rate

Various approaches can be applied to study the radon release from soil samples. In the present study, radon flux rate and radon and thoron exhalation rate were measured by using Advanced Smart Rn Duo technique developed by Bhabha Atomic Research Centre (Gaware et al. 2011). The instrument is based upon tracing the alpha (α) particles released during the decay process of $^{222}\text{Rn}/^{220}\text{Tn}$ and their progeny created due to flashing with ZnS (Ag) inside the chamber. Counts secured for each interval are converted into radon, thoron, and alpha activity concentration using a smart algorithm incorporated in the micro-controller. The scintillation detection technique for continuous measurement of radon assures many advantages over electrostatic collection-based semiconductor detectors. Since the detection concept is based on direct scintillation with ZnS(Ag), it does not have any involvement from charge negating factors (like humidity, CO_2 , and CH_4) unlike in the case of electrostatic collection-based radon detector.

Hence, Smart RnDuo does not need any additional traps (such as moisture, methane, and carbon dioxide) in the sampling passage, and its outcomes are inevitably relieved from the causes of trace gases and humidity.

Gamma spectrometry

The dried soil samples were converted into minute particles with the help of mortar and pestle after eliminating pebbles and organic substances from it. The samples were filtered with a 150- μm mesh sized strainer to make specimens homogenized. The cleaned soil samples were sealed in an impermeable cylindrical polypropylene vessel having dimensions 20.32" \times 16.51". The airtight vessels were kept at room temperature for a month; therefore, ^{226}Ra and ^{222}Rn could reach their radioactive equilibrium (Kaur et al. 2018b). Natural radioactivity of radionuclides ^{232}Th , ^{238}U , and ^{40}K in prepared soil samples was measured using thallium (Tl)-doped sodium iodide (NaI) detector. The activity of ^{238}U was calculated from the 1764 keV gamma lines of ^{214}Bi , that of ^{40}K from the 1460 keV photo peak, while that of ^{232}Th from the 2610 keV gamma lines of ^{208}Tl . The details of the method and analytical procedure are described elsewhere (Kaur et al. 2018b). The specific activity (A_s) of the nuclides is then calculated by using the following equation (Kaur et al. 2018b):

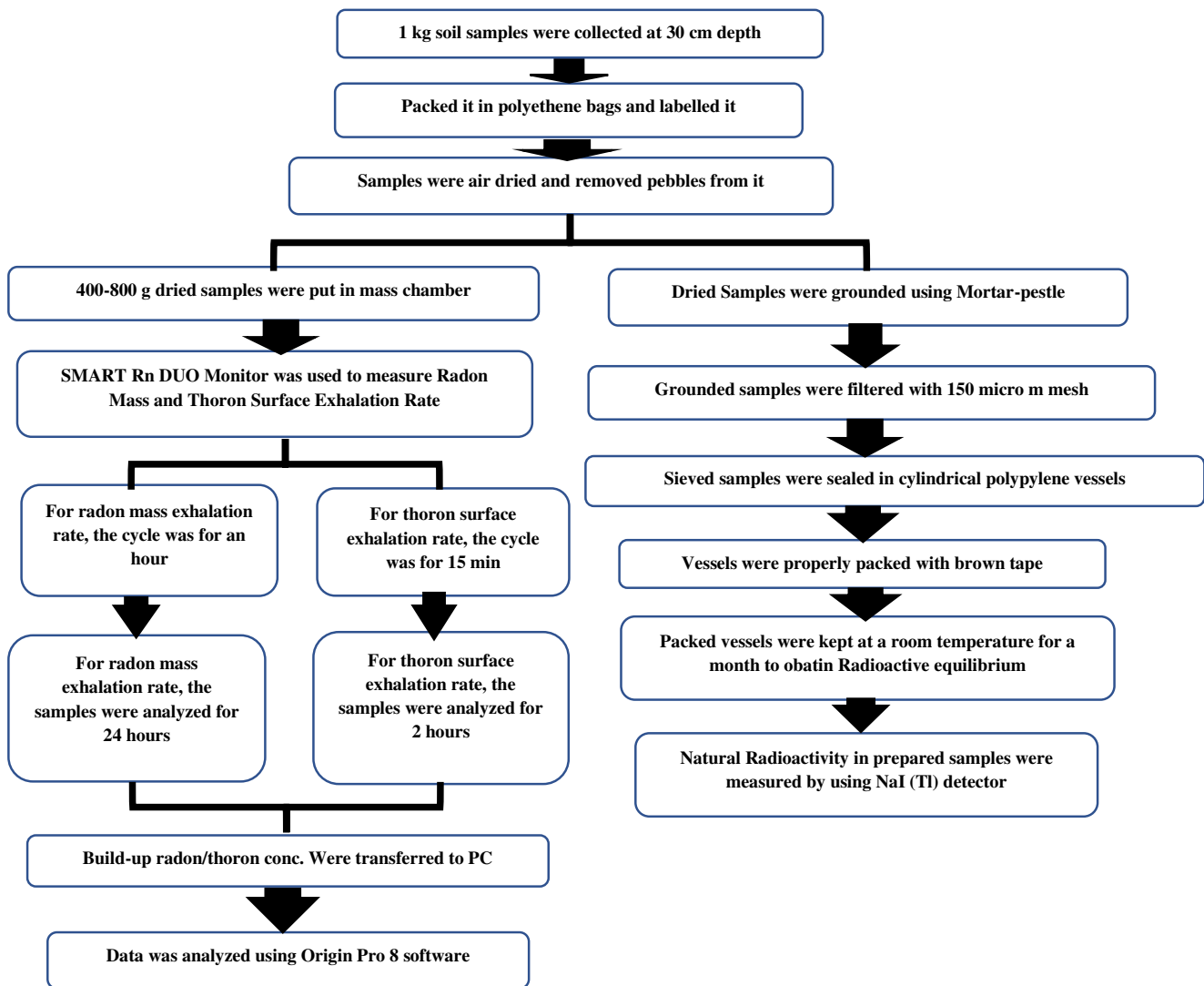


Fig. 2 Flowchart of the present research methodology

$$A_c (\text{Bqkg}^{-1}) = \frac{N_{nE}}{Y_D \times \epsilon_E \times t \times M} \quad (1)$$

The definition of the factors is provided in Table 1.

Methodology

Radon mass exhalation rate

The radon emission potential of powder sample is governed by the radon mass exhalation rate, and it can be estimated by performing measurements using Smart RnDuo of the dried soil samples (typically about 400–800g) in a mass exhalation chamber (designed for the Smart RnDuo device, height 8cm) for 24 h (Kaur et al. 2017, 2018c). Exhalation of radon concentration in

the chamber is monitored at organized meantime (i.e., 60-min cycle). The diffusion mode was used for measurements, and the chamber has been linked directly to the detector probe as described in Fig. 3. The “progeny filter” and “pinhole plate” eliminate the entry of daughter products and thoron due to “diffusion time delay” and allow only the scintillations due to radon and its daughters which are further enhanced by using a photomultiplier tube and resulted in count rate.

The radon concentration $C(T)$ at time T corresponds to accumulation inside the chamber as per the relationship (Sahoo et al. 2007):

$$C(T) = \frac{J_{Rm} m}{(V_R + (V_S \times \epsilon)) \lambda_e} [1 - e^{-\lambda_e T}] + C_0 e^{-\lambda_e T} \quad (2)$$

where the porosity (ϵ) of soil is defined as (Shiroma et al. 2015):

Table 1 Definitions and values of variable and constant factors

Variable factors	Definition	References	
A_c (Bq kg ⁻¹)	Specific activity concentration of radionuclides	Kaur et al. (2018b)	
N_{nE}	Net counts of a nuclide n in a peak at energy E	Kaur et al. (2018b)	
D	Gamma ray abundance	Kaur et al. (2018b)	
ϵ_E	Detection efficiency of the crystal	Kaur et al. (2018b)	
M (kg)	Mass of the sample for gamma spectrometry	Kaur et al. (2018b)	
J_{Rm} (Bqkg ⁻¹ h ⁻¹)	Radon mass exhalation rate	Sahoo et al. (2007)	
C_0 (Bqm ⁻³)	Radon concentration present in the chamber volume at $T=0$	Sahoo et al. (2007)	
V_s (m ³),	The soil volume	Sahoo et al. (2007)	
λ_e (h ⁻¹)	The net decay constant	Sahoo et al. (2007)	
T (h)	Calculation time	Sahoo et al. (2007)	
m (kg)	Total mass of the dry soil sample inside the chamber	Sahoo et al. (2007)	
V_R (m ³)	The effective volume, i.e., residual volume of exhalation chamber + internal volume of detector	Sahoo et al. (2007)	
ϵ	The porosity of soil	Shiroma et al. (2015):	
B (Bqm ⁻³ h ⁻¹)	Fitted slope	Sahoo et al. (2007)	
E_C (mg kg ⁻¹ for ²³⁸ U and ²³² Th; % for ⁴⁰ K)	Elemental concentration of radionuclides	UNSCEAR (2000a, 2000b, 2000c)	
$A_{M, E}$ (kg mol ⁻¹)	The atomic mass	UNSCEAR (2000a, 2000b, 2000c)	
λ_E (s ⁻¹)	Decay constant	UNSCEAR (2000a, 2000b, 2000c)	
h_E	The atomic abundance in nature	UNSCEAR (2000a, 2000b, 2000c)	
Constant factors	Definition	Values (units)	References
t	Counting time	10800 s	Kaur et al. (2018b)
ρ_g	Specific gravity of soil	2700 kg m ⁻³	Shiroma et al. (2015):
F	Factor	1,000,000 (mg kg ⁻¹) for ²³⁸ U and ²³² Th; 100 (%) for ⁴⁰ K	UNSCEAR (2000a, 2000b, 2000c)
N_{Av}	Avogadro's number	6.023×10 ²³ (atoms mol ⁻¹)	UNSCEAR (2000a, 2000b, 2000c)

Fig. 3 Setup for measurement of radon mass exhalation rate from soil sample using SMART RnDuo in diffusion mode of sampling

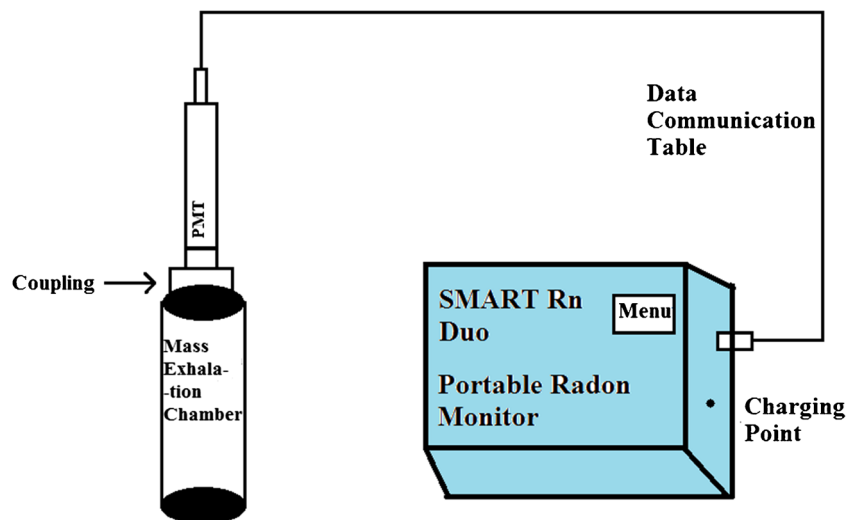




Fig. 4 Least square fitting of build-up radon concentration (Bq m⁻³) in the SMART RnDuo monitor with time (h)

$$\epsilon = 1 - \frac{m}{V_S \times \rho_g} \quad (3)$$

In linear approximation (i.e., by restricting the measurement time within 20 h), Eq. (2) can be converted to:

$$C(T) = \left[\frac{J_{Rm} m}{(V_R + (V_S \times \epsilon))} \right] T + C_0 \quad (4)$$

The build-up radon concentration inside the chamber has been transferred into the computer and has been analyzed by using OriginPro 8 software (Menon et al. 2015). Followed by least-square fitting of the data for Eq. (4), J_{Rm} from the fitted slope (Fig. 4) value has been calculated with the information of mass and residual air volume of the setup as:

$$J_{Rm} = B \left[\frac{V_R + (V_S \times \epsilon)}{m} \right] \quad (5)$$

The definition and values of the various used factors are provided in Table 1.

Thoron surface exhalation rate

Because of the low diffusion length (1–2 cm) of thoron in the air, protocols are different for evaluation of the thoron surface exhalation rate by Smart RnDuo (Gaware et al. 2011). One of the pump pipelines is linked to the flow mode sampler following a program-based sampling. The same mass exhalation chamber (height 8cm) has been used with an additional lid over it. A couple of cylindrical tubes (radius 0.25cm) were used for the circulation of air inside the chamber, and a closed-circuit loop was formed by linking the scintillation monitor to the chamber via a pump (Fig. 5). During the quarter revolution, a sampling pump was kept on for the first 5 min, which provides the assessment of background and thoron, pursuing the next 5 min, which ensures total decay of thoron, and lastly 5 min responsible for background counts. The thoron surface exhalation rate (J_{Ts}) in samples can be acquired through maintaining the content of the thoron C_T interior of the chamber with relation given by Chauhan et al. (2014).

Radon surface flux rate

In our present study, the radon emission flux rate was measured using the surface chamber (cylindrical shape accumulator) with height 15 cm and diameter 30cm and compared with the empirical and in situ method. For the measurement of radon surface flux, the edge of the accumulator has been deployed 0.5 cm deep on the soil surface (Fig. 6). The measurement has been done for about 4–5 h for a quarter rounds to analyze the escalation of radon concentration inside the accumulator volume. At the end of the measurements, build-up data on radon concentration with an elapsed time (t) was

Fig. 5 Setup for measurement of thoron surface exhalation rate from soil sample using SMART RnDuo in flow mode

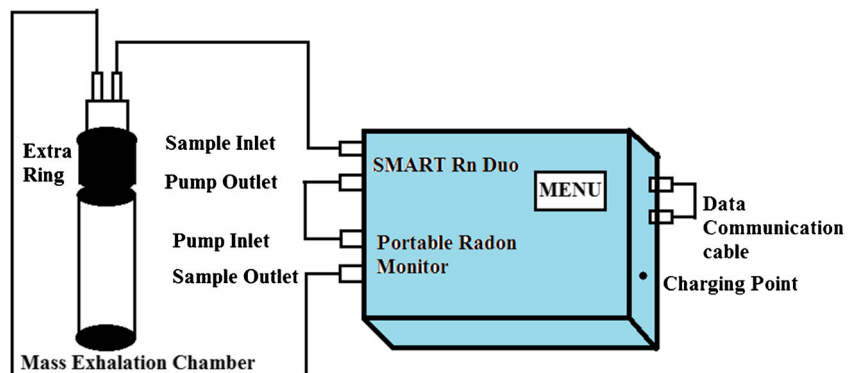
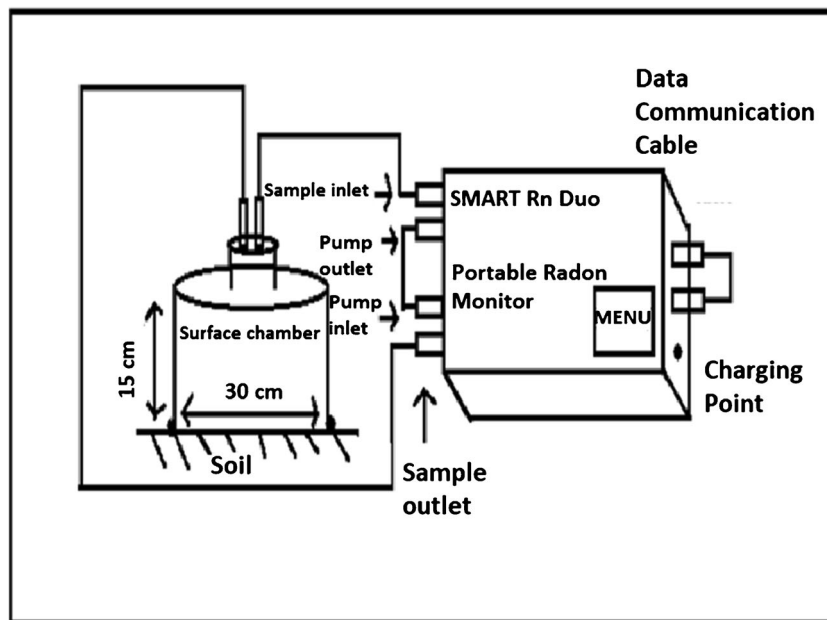


Fig. 6 Experiment setup for the measurement of radon flux ($\text{Bq m}^{-2} \text{h}^{-1}$) from the soil surface using SMART RnDuo in flow mode



retrieved, plotted, and fitted to the equation given by Sahoo et al. (2010). Followed by least-square fitting of the experimentally obtained radon accumulation values to the exponential decay equation (Sahoo et al. 2010), we can get radon surface flux rate F^m ($\text{Bq m}^{-2} \text{h}^{-1}$). The empirical F^e and in situ F^i radon surface flux rates ($\text{Bq m}^{-2} \text{h}^{-1}$) were evaluated by the process reported by researchers (Sun et al. 2004; Sahoo et al. 2010; Rogers and Nielson 1991; Zhuo et al. 2006; Nazaroff and Nero Jr. 1988).

Elemental concentration of radionuclide contents

The specific activity of ^{232}Th , ^{238}U , and ^{40}K has been transmitted into the elemental concentrations of Th (in ppm), U (in ppm), and K (in %) using the following relation (UNSCEAR 2000a, 2000b, 2000c; Celika et al. 2009):

$$EC = \frac{A_C \times A_{M,E} \times F}{\lambda_E \times N_{Av} \times h_E} \quad (6)$$

The definitions and values of various provided factors are given in Table 1. The elemental concentration of ^{238}U was determined by presuming the secular equilibrium among ^{238}U and ^{226}Ra and ^{226}Ra and ^{222}Rn .

Results and discussion

The radon mass exhalation rate was found to be varying from a minimum of 15 ± 0.4 to a maximum of 38 ± 0.8 $\text{mBq kg}^{-1} \text{h}^{-1}$ with an average value of 26 ± 6 $\text{mBq kg}^{-1} \text{h}^{-1}$ (Table 2). The thoron surface exhalation rate was found to vary from a

minimum of 90 ± 22 to maximum of 4880 ± 280 $\text{Bq m}^{-2} \text{h}^{-1}$ with an average value of 1997 ± 1040 $\text{Bq m}^{-2} \text{h}^{-1}$ (Table 2). The variation in radon mass and thoron surface exhalation rate is due to the nature of the samples, emanation factors, flux density, and porosity of the soil, respectively. The large variation of thoron surface exhalation rate in soil samples is because of assorted characteristics of rocks of the region which changes remarkably throughout the area. Relatively higher values of thoron surface exhalation rate in a few locations of hilly areas such as Nagrota (2700 ± 290 $\text{Bq m}^{-2} \text{h}^{-1}$), Nandini (4090 ± 390 $\text{Bq m}^{-2} \text{h}^{-1}$), Dansal (3260 ± 220 $\text{Bq m}^{-2} \text{h}^{-1}$), Jindrah (4880 ± 280 $\text{Bq m}^{-2} \text{h}^{-1}$), and Kishanpur (4420 ± 430 $\text{Bq m}^{-2} \text{h}^{-1}$) can be associated along the profusion of colloidal dimension division in the alluviums of upper Siwalik.

The median values of radon mass exhalation rate and thoron surface exhalation rate are 28 ± 6 $\text{mBq kg}^{-1} \text{h}^{-1}$ and 1755 ± 1040 $\text{Bq m}^{-2} \text{h}^{-1}$, respectively. The larger mean value of the thoron surface exhalation rate than the median value indicated that the distribution is positively skewed. The value of kurtosis and skewness also specifies that the dispensation is log-normal. In the case of radon mass exhalation rate, the mean value is comparatively equal to the median value, clearing that the distribution is normal. The normal distribution of radon mass exhalation rate is also depicted by the values of skewness and kurtosis.

The Shapiro-Wilk (SW) (Shapiro and Wilk 1965) test was also implied to study the normality of the radon mass and thoron surface exhalation rate. In the case of radon mass exhalation rate, the Shapiro-Wilk test presented a test static of 0.91 along 0.22 as a p value, and for thoron surface exhalation rate, the p value was 0.01 along 0.93 as a test static. The p

Table 2 Measurement of exhalation rate and specific activity of radionuclide content in soil samples of Jammu district

Sr. no.	Villages	Exhalation rate		Radionuclide contents (Bq kg ⁻¹)			Elemental concentration		
		Radon mass (mBq kg ⁻¹ h ⁻¹)	Thoron surface (Bqm ⁻² h ⁻¹)	A _U	A _{Th}	A _K	E _U (mg kg ⁻¹)	E _{Th} (mg kg ⁻¹)	E _K (%)
1.	Mehmood Pura	17±0.6	1090±230	27±10	21±7	192±13	2.2	5	0.58
2.	Kotlimian	22±0.8	2150±290	14±7	24±7	329±19	1.1	6	0.98
3.	Darsopur	32±1.2	1430±240	30±10	27±6	359±20	2.4	7	0.78
4.	Miran Sahib	18±1.1	1400±220	27±11	37±8	315±20	2.2	9	0.94
5.	Lalle da bagh	28±0.8	1600±300	22±9	28±7	299±20	1.8	7	0.90
6.	Ghou manasa	16±0.7	1400±340	10±7	23±5	186±15	0.8	5	0.56
7.	Marh	30±0.7	1770±300	31±10	33±8	305±21	2.5	8	0.91
8.	Bindra da bagh	21±0.7	990±200	23±11	20±7	311±20	1.9	5	0.93
9.	Baazigar basti	21±1.0	1130±210	20±8	24±7	340±20	1.6	6	1.02
10.	Sua no.1	24±0.3	2030±260	20±10	22±8	282±19	1.6	5	0.85
11.	Bhalwan bhamna	21±0.8	2080±360	19±9	41±8	322±21	1.5	10	0.97
12.	Dok khalsa	27±1.1	2000±290	17±10	49±8	376±20	1.4	12	1.12
13.	Panyali	23±0.8	1080±200	21±9	17±5	246±20	1.7	4	0.74
14.	Kharah	15±0.4	1010±180	14±6	21±7	306±20	1.1	5	0.92
15.	Chak malal	16±0.7	90±22	19±9	18±5	287±15	1.5	4	0.86
16.	Nagrota	30±0.8	2700±290	37±10	49±7	486±20	3.0	12	1.46
17.	Nandini	36±1.0	4090±390	32±9	58±8	513±21	2.6	14	1.54
18.	Dansal	28±0.8	3260±220	33±9	53±7	350±20	2.7	13	1.05
19.	Jindrah	33±0.8	4880±280	39±10	70±7	211±19	3.2	17	0.63
20.	Kishanpur	38±0.8	4420±430	40±10	58±8	323±20	3.2	14	0.97
21.	Suchetgarh	26±1.0	1860±300	28±8	29±8	395±21	2.3	7	1.18
22.	Agore	28±1.1	2390±310	33±10	38±9	332±20	2.7	9	1.00
23.	Amb	29±1.0	1700±310	28±9	41±8	379±20	2.3	10	1.14
24.	Kot	24±0.7	1170±320	24±9	43±8	374±20	1.9	10	1.12
25.	Bantalab	32±1.2	1740±660	21±9	16±7	143±15	1.7	4	0.43
26.	Mishriwala	31±1.0	2520±420	16±10	37±8	381±20	1.3	9	1.14
27.	Patoli	29±0.7	2480±360	23±9	38±8	177±15	1.9	9	0.53
28.	New rehari	29±1.0	1430±220	26±9	37±8	297±19	2.1	9	0.89
29.	Kalith	29±1.2	1440±360	18±8	26±9	509±21	1.5	6	1.53
30.	Pallanwala	17±0.5	2590±330	19±8	47±9	406±20	1.5	11	1.22
Min.		15	90	10	16	143	0.8	4	0.43
Max.		38	4880	40	70	513	3.2	17	1.54
Average		26	1997	24	35	324	2.0	8	0.96
S.D.*		6	1040	8	14	89	0.6	3	0.27
G.M.**		25	1690	23	32	311	1.9	8	0.92
Median		28	1755	23	35	323	1.9	8	0.95
Kurtosis		-0.8	1.5	-0.5	-0.2	0.3	-0.5	-0.2	0.21
Skewness		-0.1	1.2	0.3	0.6	0.1	0.3	0.7	0.23

*standard deviation; **geometric mean

value in the case of radon mass exhalation rate is greater than 5%; therefore, the test credited the presumption of normality. On the other hand, the *p* value of the thoron surface exhalation rate is smaller than 5%; therefore, the test rejects the

hypothesis of normality. The SW test is in agreement with the values of standardized skewness and kurtosis.

In the present appraisal, the observed results of radon mass exhalation rate were higher as compared to Mohali, Punjab, Northern India (0.3 to 3 mBq kg⁻¹ h⁻¹) (Mehta et al. 2015),

Southern Punjab (1 to 9 mBq kg⁻¹ h⁻¹) (Mujahid et al. 2010), and Azad Kashmir (5 to 10 mBq kg⁻¹ h⁻¹) (Rafique et al. 2011) of Pakistan. The observed values of radon mass exhalation rate in the analyzed samples were in general comparable to the values of Kangra district (15 to 35 mBq kg⁻¹ h⁻¹) (Sharma et al. 2003) and Nurpur area (15 to 35 mBq kg⁻¹ h⁻¹) (Singh et al. 2007) of Himachal Pradesh and Udhampur area (6 to 22 mBq kg⁻¹ h⁻¹) (Kumar et al. 2009) and Ganderbal district (5 to 22 mBq kg⁻¹ h⁻¹) (Mir and Rather 2015) of Jammu and Kashmir Himalayas. However, the analyzed values were quite lower than that of Hamirpur district (10 to 54 mBq kg⁻¹ h⁻¹) (Singh et al. 2016) perhaps owing to leaching (Kaul et al. 1993) of radioactive components through the uranium upgraded province of the Himachal Himalayas. The values of the present investigation are also lower than those of five surveyed districts (28 to 91 mBq kg⁻¹ h⁻¹) of Northern Haryana (Chauhan et al. 2014), as these districts are covered by the segment of the Shivalik mountains along the Yamuna river; stream contains sand blend soil which has generally high radionuclide content.

The values of radon mass exhalation (15 to 38 mBq kg⁻¹ h⁻¹) were also compared with worldwide data. Ielsch et al. (2002) have reported a radon mass exhalation range of 0.3 to 25 mBq kg⁻¹ h⁻¹ in soil samples of France. Saad et al. (2013) have reported a radon mass exhalation range of 1.2 to 61 mBq kg⁻¹ h⁻¹ in Libyan soil samples. Tabar et al. (2016) have reported the range of 36 to 253 mBq kg⁻¹ h⁻¹ for radon mass exhalation rate in soil samples of southern Sakarya, Turkey. The range of radon mass exhalation was 8 to 234 mBq kg⁻¹ h⁻¹ for the soil samples of Alexandria city, Egypt (El-Zaher 2013).

UNSCEAR (2000a) report and Prajith et al. (2019) have showed that the worldwide average of the thoron surface exhalation rates is 3600 Bq m⁻² h⁻¹. The obtained mean value in the survey was much lower than the value of UNSCEAR (2000a) report, and most thoron exhalation rate values (about

90%) were within the global average value recommended by UNSCEAR (2000a) report. Only 10% of values (3 samples) were found above the world average.

Table 3 lists the various parameters used during the calculation of in situ measured flux rate and exhalation rate measured on soil samples. Table 3 depicted the range, average, standard deviation, and geometric mean of measured, empirical, and in situ radon fluxes from soil surface which shows that in situ and measured values of radon flux were almost same as compared to the empirical radon flux. This may be attributed due to the estimation of the radon flux rate from direct measurement, and in situ measurement was from the same soil profile. Figure 7 shows the correlation observed in the radon mass exhalation rate (Bq kg⁻¹ h⁻¹) with measured (correl coeff. = 0.58), in situ (correl coeff. = 0.77), and empirical (correl coeff. = 0.18) radon flux rates (Bq m⁻² h⁻¹).

The Mann-Whitney test was exercised under the null presumption that the medians of the radon flux rate for the measured, in situ, and empirical methods are the same (Mann and Whitney 1947). The Mann-Whitney test (1947) presented statistically noteworthy contrasts in the medians of the radon flux rate ($Z = -6.6; p=0.000 < 0.001$) for measured, in situ, and empirical methods, respectively.

The world average specific activity is 35, 30, and 400 Bq kg⁻¹ for ²³⁸U, ²³²Th, and ⁴⁰K, respectively, reported in UNSCEAR (2000a). The average activity concentration of ²³⁸U is 24 ± 8 Bq kg⁻¹ with a range of 10 ± 7 Bq kg⁻¹ (sample collected at Ghou Manasa) to 40 ± 10 Bq kg⁻¹ (sample collected at Kishanpur), and the average activity concentration of ²³²Th is 35 ± 14 Bq kg⁻¹ with a range of 16 ± 7 Bq kg⁻¹ (sample collected at Bantalab) to 70 ± 7 Bq kg⁻¹ (sample taken at Jindrah) as given in Table 2. The arithmetic mean ± SD range of ⁴⁰K series concentration was estimated to be 324 ± 89, 143 ± 15 (sample collected from Bantalab), and 513 ± 21 Bq kg⁻¹ (sample collected from Nandini), respectively. The value of thoron concentration in fourteen soil samples

Table 3 Soil parameters in collected soil samples of Jammu district, Jammu and Kashmir, India

Parameters	Minimum	Maximum	Average ± S.D.	G.M.
Uranium content, A _U (Bq kg ⁻¹)	10	40	24±8	23
In situ ²²² Rn diffusive length, l _s (m)	0.62	0.96	0.76±0.10	0.76
In situ ²²² Rn emanation factor E	0.05	0.49	0.18±0.10	0.16
Dry ²²² Rn emanation factor E ₀	0.06	0.16	0.10±0.03	0.10
Density, ρ (kg m ⁻³)	1011	1887	1336±192	1323
Porosity, C	0.37	0.59	0.47±0.05	0.46
Moisture saturation, m	0.2	0.74	0.48±0.16	0.45
Temperature, T (K)	300	466	375±54	371
In situ radon flux rate, F ⁱ (Bqm ⁻² h ⁻¹)	16	36	26±6	24
Measured radon flux rate, F ^m (Bqm ⁻² h ⁻¹)	19	46	30±6	28
Empirical radon flux rate, F ^e (Bqm ⁻² h ⁻¹)	16	88	49±19	45

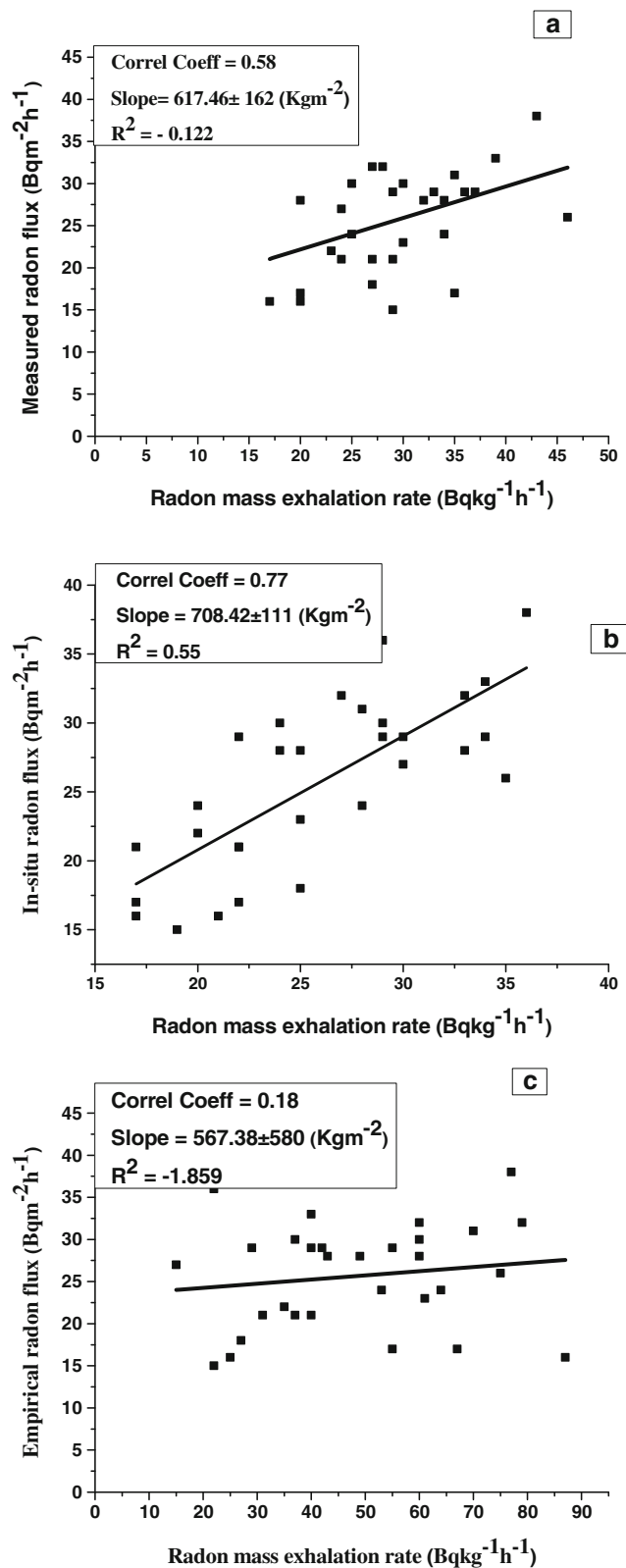


Fig. 7 Correlation observed for radon mass exhalation rate ($\text{Bq kg}^{-1} \text{h}^{-1}$) with **a** measured radon flux ($\text{Bq m}^{-2} \text{h}^{-1}$), **b** in situ radon flux ($\text{Bq m}^{-2} \text{h}^{-1}$), and **c** empirical radon flux ($\text{Bq m}^{-2} \text{h}^{-1}$)

(47%) and the value of potassium concentration in twenty-six soil samples (87%) were found within the world average values suggested by UNSCEAR (2000a). However, the concentration of ^{238}U is very much comparable to world concentration. Relatively elevated values of ^{232}Th and ^{40}K in soil samples as compared to global mean perhaps correspond to the fact that the soil of that region is thorium and potassium rich. The measured values of radionuclide contents, i.e., ^{238}U , ^{232}Th , and ^{40}K of the present study, are also compared with worldwide research data (Table 4).

Ramola et al. (2014) have reported the range of ^{238}U , ^{232}Th , and ^{40}K as 8–285 Bq kg^{-1} , 7–136 Bq kg^{-1} , and 115–1588 Bq kg^{-1} in the Garhwal Himalayas, India. Bala et al. (2014) have reported the range of ^{238}U , ^{232}Th , and ^{40}K as 36.4–51.9 Bq kg^{-1} , 9.3–26.1 Bq kg^{-1} , and 1361–1732 Bq kg^{-1} in Una, Himachal Pradesh, India. The range of ^{238}U , ^{232}Th , and ^{40}K has been varied from 26.02 to 93.54 Bq kg^{-1} , 29.34 to 114.41 Bq kg^{-1} , and 348.15 to 752.98 Bq kg^{-1} in Punjab Province, Pakistan, cited by Rahman et al. (2011). Also, Rahman et al. (2009) cited the range of ^{238}U , ^{232}Th , and ^{40}K from 415 to 106.2 Bq kg^{-1} , 4 to 193.8 Bq kg^{-1} , and 325.3 to 657.4 Bq kg^{-1} in Islamabad, Pakistan. Badhan and Mehra 2012 have reported the range of ^{238}U , ^{232}Th , and ^{40}K from 23.56 to 34.07 Bq kg^{-1} , 41.98 to 63.07 Bq kg^{-1} , and 432.98 to 800.09 Bq kg^{-1} in the soil samples of Ludhiana, India. The range of ^{238}U , ^{232}Th , and ^{40}K has been varied from 2.26 to 30.57 Bq kg^{-1} , 6 to 93.64 Bq kg^{-1} , and 39.81 to 551.72 Bq kg^{-1} in the soil samples of Mining Area, Ghana, cited by Faanu et al. (2011). Abdallah et al. (2017) have reported the range of ^{238}U , ^{232}Th , and ^{40}K from 7.75 to 250 Bq kg^{-1} , 4 to 88 Bq kg^{-1} , and 75 to 359 Bq kg^{-1} in sediments of River Nile, Egypt. The range of ^{238}U , ^{232}Th , and ^{40}K has been varied from 16 to 102 Bq kg^{-1} , 21 to 90 Bq kg^{-1} , and 184 to 979 Bq kg^{-1} in the soil samples of Southern Serbia reported by Sarap et al. (2014). Hassan et al. (2010) reported the range of ^{238}U , ^{232}Th , and ^{40}K from 0.8 to 320 Bq kg^{-1} , 0.4 to 200 Bq kg^{-1} , and 1 to 1100 Bq kg^{-1} in Japan. Gussain et al. (2012) have reported the range of ^{238}U , ^{232}Th , and ^{40}K from 15.6 to 69 Bq kg^{-1} , 28.9 to 973 Bq kg^{-1} , and 39 to 952 Bq kg^{-1} in Odisha, India. Rani et al. (2015) have reported the range of ^{238}U , ^{232}Th , and ^{40}K from 13 to 36 Bq kg^{-1} , 40 to 71 Bq kg^{-1} , and 294 to 781 Bq kg^{-1} in the soil samples of Rajasthan, India. Gulan et al. (2013) have reported the range of ^{238}U , ^{232}Th , and ^{40}K from 21.2 to 91.1 Bq kg^{-1} , 20.3 to 103.8 Bq kg^{-1} , and 365.1 to 1148.7 Bq kg^{-1} in North Kosovska, Europe. Asaduzzaman et al. (2015) have reported the range of ^{238}U , ^{232}Th , and ^{40}K from 49.4 to 60.5 Bq kg^{-1} , 64.7 to 82 Bq kg^{-1} , and 927.2 to 1080.3 Bq kg^{-1} in Bangladesh. Al-Jundi et al. (2005) have reported the range of ^{238}U , ^{232}Th , and ^{40}K from 27.7 to 70.4 Bq kg^{-1} , 5.9 to 32.9 Bq kg^{-1} , and 30.8 to 58.5 Bq kg^{-1} in Jordan.

The activity of ^{238}U , ^{232}Th , and ^{40}K follows the normal distribution as the values of the means are approximately

Table 4 Comparison of measured present values of radionuclide contents with worldwide data

Regions	A _U (Bq kg ⁻¹)	A _{Th} (Bq kg ⁻¹)	A _K (Bq kg ⁻¹)	References
Garhwal Himalaya, India	8–285	7–136	115–1588	Ramola et al. (2014)
Una, Himachal Pradesh, India	36.4–51.9	9.3–26.1	1361–1732	Bala et al. (2014)
Punjab Province, Pakistan	26.02–93.54	29.34–114.41	348.15–752.98	Rahman et al. (2011)
Islamabad, Pakistan	41.5–106.2	4.0–193.8	325.3–657.4	Rahman et al. (2009)
Ludhiana, India	23.56–34.07	41.98–63.07	432.98–800.09	Badhan et al. (2012)
Mining Area, Ghana	2.26–30.57	6–93.64	39.81–551.72	Faanu et al. (2011)
River Nile, Egypt	7.75–250	4–88	75–359	Abdellah et al. (2017)
Southern Serbia	16–102	21–90	184–979	Sarap et al. (2014)
Japan	0.8–320	0.4–200	1–1100	Hassan et al. (2010)
Odisha, India	15.6–69	28.9–973	39–952	Gusain et al. (2012)
Rajasthan, India	13–36	40–71	294–781	Rani et al. (2015)
North Kosovska Mitrovica, Europe	21.2–91.1	20.3–103.8	365.1–1148.7	Gulan et al. (2013)
Bangladesh	49.4–60.5	64.7–82.0	927.2–1080.3	Asaduzzaman et al. (2015)
Jordan	27.7–70.4	5.9–32.9	30.8–58.5	Al-Jundi et al. (2005)
Jammu, India	10–40	16–70	143–513	Present study

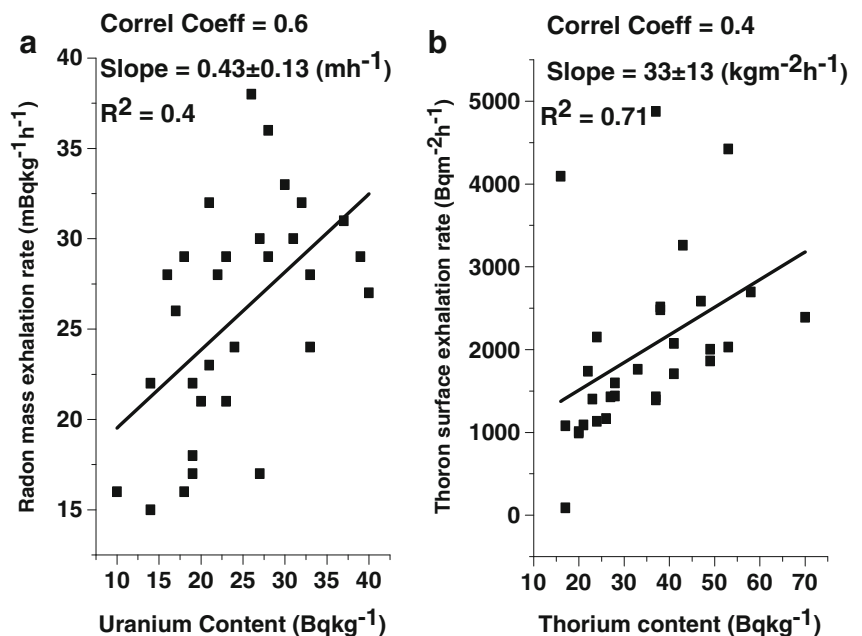
equal to the median values. The values of skewness and kurtosis are 0.3 Bq kg⁻¹ and -0.5 Bq kg⁻¹ for ²³⁸U activity; 0.7 Bq kg⁻¹ and -0.2 Bq kg⁻¹ for ²³²Th activity; and 0.1 Bq kg⁻¹ and 0.3 Bq kg⁻¹ for ⁴⁰K activity, respectively. This also follows the trend of normal distribution.

The elemental concentration of ²³⁸U, ²³²Th, and ⁴⁰K was fluctuating between 0.8 and 3.2 mg kg⁻¹; 4 and 17 mg kg⁻¹; and 0.43 and 1.54% (Table 2). The mean values of elemental concentration were 2.0 ± 0.6 mg kg⁻¹; 8 ± 3 mg kg⁻¹; and 0.96

± 0.27%, respectively. The average elemental concentration of ²³⁸U and ⁴⁰K was found to be well within the mean values (2.8 mg kg⁻¹ and 1.3%) published by UNSCEAR (2000a). However, the mean elemental value of ²³²Th was found comparable with the global average value (7.4 mg kg⁻¹) given by UNSCEAR (2000a).

Figure 8a shows the correlation between the uranium activity and the radon mass exhalation rate and found a positive correlation coefficient of 0.6. Similarly, the correlation factor

Fig. 8 Correlation observed between **a** radon mass exhalation rate (mBq kq⁻¹ h⁻¹) and uranium content (Bq kg⁻¹) and **b** thoron surface exhalation rate (Bq m⁻² h⁻¹) and thorium content (Bq kg⁻¹)



was observed between thorium activity and thoron surface exhalation rate and found a positive and weak correlation coefficient of 0.4 in Fig. 8b. Overall, thoron exhalation rate values were found higher than the recommended limit in most of the villages due to highly thorium-rich soil in the present study.

Assessment of radiological hazards

The measured specific activity was used to estimate the radiological hazards associated with the soil of the studied area to demonstrate an effective conclusion for the health status of the inhabitants living in that area. To assess the radiation hazards associated with the studied soil samples, the following nine quantities have been studied.

Radium equivalent activity (Ra_{eq})

The radium equivalent activity (Ra_{eq}) in $Bq\ kg^{-1}$ was proposed to define homogeneity with respect to radiation exposure (OECD 2009) and to assess the radiation hazards originating due to the consumption of the soil in the construction of buildings. This radium equivalent activity represents a weighted summation of activities of ^{40}K , ^{238}U , and ^{232}Th radionuclides and is based on the estimation that $370\ Bq\ kg^{-1}$ of ^{238}U , $259\ Bq\ kg^{-1}$ of ^{232}Th , and $4810\ Bq\ kg^{-1}$ of ^{40}K produce the same radiation dose rates. It is calculated by the following equation (UNSCEAR 2000a):

$$Ra_{eq} = 370 \left(\frac{A_U}{370} + \frac{A_{Th}}{259} + \frac{A_K}{4810} \right) \quad (7)$$

$$\Rightarrow Ra_{eq} = A_U + 1.43A_{Th} + 0.077A_K$$

where A_U , A_{Th} , and A_K are the specific activities ($Bq\ kg^{-1}$) of ^{238}U , ^{232}Th , and ^{40}K , respectively, in the soil samples. The calculated value of radium equivalent activity fluctuated between 55 and $159\ Bq\ kg^{-1}$ along a mean of $99 \pm 27\ Bq\ kg^{-1}$ and is given in the third column of Table 5. All observed values have shown Ra_{eq} activities lower than the limit set by the OECD 2009 report ($370\ Bq\ kg^{-1}$), equivalent to an external gamma dose of $1.5\ mSv\ a^{-1}$. Hence it does not bring about any health hazards to the population of a reviewed region.

External and internal health effects

The external and internal health consequences caused by the existence of radionuclides in the soil are prescribed by the relation (Beretka and Mathew 1985; Bala et al. 2014; Ramola et al. 2014):

$$H_{ex} = \frac{A_U}{370Bqkg^{-1}} + \frac{A_{Th}}{259Bqkg^{-1}} + \frac{A_K}{4810Bqkg^{-1}} \leq 1 \quad (8)$$

$$H_{in} = \frac{A_U}{185Bqkg^{-1}} + \frac{A_{Th}}{259Bqkg^{-1}} + \frac{A_K}{4810Bqkg^{-1}} \leq 1 \quad (9)$$

Table 3 shows the mean value of 0.27 ± 0.07 for H_{ex} with a range of 0.53 to 0.43. It is found to be below the criterion value (<1) (UNSCEAR 2000a; 1993). The values of this index must be less than unity if the radiation hazard is to be considered insignificant. An average value of H_{in} is determined to be 0.33, which is <1 as shown in the fifth column of Table 5, indicating that the internal hazard is below the critical value. It indicates that the soil samples are free from radiation hazards.

Absorbed dose rate (ADR)

Effects of gamma radiation are often expressed in terms of the absorbed dose rate in air, which originates from radionuclides in the soil. It is noteworthy in the radiation threat analysis as it quantifies the amount of rate of radiation deposited. The gamma absorbed dose rates are evaluated applying equation written below:

$$ADR(nGyh^{-1}) = 0.604A_{Th} + 0.462A_U + 0.0417A_K \quad (10)$$

where the numerical factors are the conversion factors from $Bq\ kg^{-1}$ to $nGy\ h^{-1}$ (UNSCEAR 2000a). From Eq. (10), the dose contribution per unit activity concentration of ^{232}Th to ^{238}U to ^{40}K is in the ratio of 1:0.8:0.07. The gamma absorbed doses in air ranged between 25 and $71\ nGyh^{-1}$ with an average of $47 \pm 12\ nGyh^{-1}$. Of the soil samples, 87% were within the world average value published by UNSCEAR (2000a), i.e., $60\ nGyh^{-1}$; hence the study area is posing no radiation hazard to the human population of the studied area.

Annual effective dose equivalent (AEDE)

To make a rough approximation of the annual ambient dose, one has to take into account the transformation factor for effective dose through absorbed dose and the outdoor occupancy factor (Bala et al. 2014; Ramola et al. 2014; Singh et al. 2016; UNSCEAR 2000a):

$$AEDE\ (Indoor)\ (\mu Sv\ a^{-1}) = ADR\ (nGyh^{-1}) \times T(In_{exp}) \times OF_{In} \times Dose_{CF} \times 10^{-3} \quad (11)$$

$$AEDE\ (Outdoor)\ (\mu Sv\ a^{-1}) = ADR\ (nGyh^{-1}) \times T(Out_{exp}) \times OF_{Out} \times Dose_{CF} \times 10^{-3} \quad (12)$$

where $T(In_{exp})$ and $T(Out_{exp})$ are the indoor and outdoor rates of exposure duration, i.e., $7000\ h\ a^{-1}$ and

Table 5 Measured values of $R_{a_{eq}}$, CF, H_{ex} , H_{in} , I_{γ} , I_{α} , absorbed dose rate, annual effective dose, excess lifetime cancer risk, and annual gonad equivalent dose in studied soil samples collected from Jammu district

Sr. no.	Name of villages	$R_{a_{eq}}$ (Bqkg ⁻¹)	$H_{ex} \leq 1$	$H_{in} \leq 1$	ADR (nGyh ⁻¹)	AEDE(μ Sva ⁻¹)		AGED (μ Sva ⁻¹)
						Indoor	Outdoor	
1	Mehmood pura	72	0.20	0.27	33	130	8	232
2	Kotlimian	74	0.20	0.24	35	136	9	247
3	Darsopur	98	0.27	0.35	46	181	11	325
4	Miran sahib	104	0.28	0.35	48	188	12	337
5	Lalle da bagh	85	0.23	0.29	40	155	10	279
6	Ghou manasa	57	0.15	0.18	26	103	7	185
7	Marh	102	0.27	0.36	47	184	12	330
8	Bindra da bagh	76	0.20	0.27	36	140	9	252
9	Baazigar basti	80	0.22	0.27	38	149	9	269
10	Sua no. 1	130	0.35	0.44	59	231	15	412
11	Bhalwan bharmna	102	0.28	0.33	47	184	12	331
12	Dok khalsa	139	0.38	0.48	64	250	16	447
13	Panyali	64	0.17	0.23	30	119	8	213
14	Kharah	66	0.18	0.22	31	123	8	223
15	Chak Malal	64	0.17	0.22	31	120	8	217
16	Nagrota	88	0.24	0.29	42	166	10	303
17	Nandini	111	0.30	0.35	52	205	13	373
18	Jindrah	69	0.19	0.23	32	125	8	224
19	Dansal	97	0.26	0.34	45	177	11	320
20	Kishanpur	140	0.38	0.48	63	249	16	443
21	Suchetgarh	128	0.35	0.42	59	231	15	415
22	Agore	159	0.43	0.52	71	280	18	499
23	Amb	116	0.31	0.39	54	210	13	377
24	Kot	114	0.31	0.37	53	206	13	371
25	Bantalab	55	0.15	0.20	25	99	6	177
26	Mishriwala	119	0.32	0.42	55	217	14	389
27	Patoli	91	0.25	0.31	41	161	10	286
28	New rehari	102	0.27	0.35	47	183	12	328
29	Kalith	141	0.38	0.43	65	255	16	461
30	Pallanwala	117	0.31	0.36	54	210	13	380
Minimum		55	0.15	0.18	25	99	6	177
Maximum		159	0.43	0.52	71	280	18	499
Average		99	0.27	0.33	47	179	11	321
S.D.		27	0.07	0.09	12	47	3	84
G.M.		95	0.26	0.32	44	172	11	310

1760 h a⁻¹; OF_{Out} and OF_{In} are an occupancy factor for outdoor (0.2) and indoor (0.8) effective dose; and Dose_{CF} is an effective dose of the absorbed dose conversion factor (0.7 Sv Gy⁻¹). The present value of outdoor and indoor annual effective dose equivalent is lower than the world average values of 70 μ Sv a⁻¹ for outdoor and 450 μ Sv a⁻¹ for indoor as tabulated in the seventh and eighth column of Table 5 (Ramola et al. 2014; Singh et al. 2016; UNSCEAR 1993).

Annual gonad equivalent dose (AGED)

The gonads, the activity of bone marrow, and the bone surface cells are considered as organs of interest (UNSCEAR 1988) because these are the most sensitive parts of the human body when exposed to radiation. To determine the exposure caused by radiation to sensitive parts of the human body, an annual gonad equivalent dose has been calculated as (Barreyni Toossi et al.

2009; Darwin et al. 2015; Raghu et al. 2016; UNSCEAR 1988):

$$\text{AGED } (\mu\text{Sv a}^{-1}) = 3.09A_{\text{U}} + 4.18A_{\text{Th}} + 0.314A_{\text{K}} \quad (13)$$

where the numerical factors are the conversion factors from Bq kg^{-1} to $\mu\text{Sv a}^{-1}$ (UNSCEAR 1988). The average value of the annual gonad equivalent dose was found below the permissible values of $300\mu\text{Sv a}^{-1}$ (UNSCEAR 2000a). This depicts that the gonad values produce no danger to the bone marrow and the bone surface cells of the inhabitants exploring soil in the study area.

Conclusions

The average radon mass exhalation rate and thoron surface exhalation rate were measured as $26 \pm 6 \text{ mBq kg}^{-1} \text{ h}^{-1}$ and $1997 \pm 1040 \text{ Bq m}^{-2} \text{ h}^{-1}$. The resulted values of radon mass exhalation rate are comparable to the values of the Nurpur area and Kangra district of Himachal Pradesh and Ganderbal district and Udhampur district of Jammu and Kashmir. The resulted values of radon mass exhalation rate were found to be lower than global values reported by researchers (Kaul et al. 1993; Saad, Abdallah and Hussain 2013; Singh et al. 2016). In a few locations, the calculated thoron surface exhalation rate values were slightly higher than the recommended value given by UNSCEAR (2000a) due to the profusion of colloidal dimension division in the alluviums of upper Siwalik. It is also observed that the distribution of the thoron surface exhalation rate was log-normal, while the distribution of radon mass exhalation rate was normal. In situ measured flux rate and exhalation rate measured on soil samples values were found in good agreement with the radon mass exhalation rate as compared to the calculated based on empirical equation. The average activity concentration of ^{238}U , ^{232}Th , and ^{40}K were $24 \pm 8 \text{ Bq kg}^{-1}$, $35 \pm 14 \text{ Bq kg}^{-1}$, and $324 \pm 89 \text{ Bq kg}^{-1}$, respectively. The range of uranium concentration is comparable to worldwide values, but the concentration of thorium and potassium was found slightly higher than worldwide values due to thorium- and potassium-rich soil of the present study. A positive but very weak correlation has been found between the radon mass exhalation rate and uranium concentration in soil. All measured radiological hazards were found within their world average values, and hence the results revealed that the study sites are safe from a health perspective from the studied hazardous effects of radon and natural radioactivity.

Acknowledgements Authors are grateful to the Department of Atomic Energy, BRNS (Mumbai), for aiding the grant under the major research project (Sanction no. 2013/36/60-BRNS) for this work. Authors are also highly grateful to DAV College, Amritsar, and NIT, Jalandhar, for their

support in carrying out the experimental work. Our sincere thanks to the inhabitants of the studied area for their cooperation during the field work.

Declarations

Conflict of interest The author(s) declare that they have no competing interests.

References

- Abdellah WM, Diab HM, El-Kameesy SU, Salama E, El-Framawy S (2017) Natural radioactivity levels and associated health hazards from the terrestrial ecosystem in Rosetta branch of the River Nile, Egypt. *Isot Environ Health Stud* 53(4):427–439. <https://doi.org/10.1080/10256016.2017.1293668>
- Abumurad KM, Al-Tamimi M (2001) Emanation power of radon and its concentration in soil and rocks. *Radiat Meas* 34:423–426. [https://doi.org/10.1016/S1350-4487\(01\)00199-8](https://doi.org/10.1016/S1350-4487(01)00199-8)
- Agbalagba EO, Onoja RA (2011) Evaluation of natural radioactivity in soil, sediment and water samples of Niger Delta (Biseni) Flood Plain Lakes, Nigeria. *J Environ Radioact* 102:667–671. <https://doi.org/10.1016/j.jenvrad.2011.03.002>
- Al-Jundi J, Salah W, Bawa'aneh MS, Afaneh F (2005) Exposure to radiation from the natural radioactivity in Jordanian building materials. *Radiat Prot Dosim* 118(1):93–96. <https://doi.org/10.1093/rpd/nci332>
- Al-Jundia J, Al-Bataina BA, Abu-Rukah Y, Shehadeh HM (2003) Natural radioactivity concentrations in soil samples along the Amman Aqaba Highway, Jordan. *Radiat Meas* 36:555–560. [https://doi.org/10.1016/S1350-4487\(03\)00202-6](https://doi.org/10.1016/S1350-4487(03)00202-6)
- Asaduzzaman K, Mannan F, Khandaker MU, Farook MS, Elkezza A, Mohd Amin YB, Sharma S, Kassim HBA (2015) Assessment of natural radioactivity levels and potential radiological risks of common building materials used in Bangladesh. *PLoS One* 10(10): e0140667. <https://doi.org/10.1371/journal.pone.0140667>
- Badhan K, Mehra R (2012) Primordial Radioactivity (^{238}U , ^{232}Th , and ^{40}K) Measurements for soils of Ludhiana District of Punjab, India. *Radiat Prot Dosim* 152:1–4. <https://doi.org/10.1093/rpd/ncs144>
- Bala P, Mehra R, Ramola RC (2014) Distribution of natural radioactivity in soil samples and radiological hazards in building material of Una, Himachal Pradesh. *J Geochem Explor* 142:11–15. <https://doi.org/10.1016/j.gexplo.2014.02.010>
- Beretka J, Mathew PJ (1985) Natural radioactivity of Australian building materials, industrial wastes and by-products. *Health Phys* 48:87–95
- Celika N, Cevik U, Celik A, Koz B (2009) Natural and artificial radioactivity measurements in Eastern Black Sea region of Turkey. *J Hazard Mater* 162:146–153. <https://doi.org/10.1016/j.jhazmat.2008.05.017>
- Chauhan RP, Kumar A, Chauhan N, Joshi M, Aggarwal P, Sahoo BK (2014) Ventilation effect on indoor radon–thoron levels in dwellings and correlation with soil exhalation rates. *Indoor Built Environ* 25: 203–212. <https://doi.org/10.1177/1420326X14542887>
- Darwin DAE, Abul-Nasr KTM, AM EL-K (2015) The assessment of natural radioactivity and its associated radiological hazards and dose parameters in granite samples from South Sinai, Egypt. *J Radiat Res Appl Sci* 8(1):17–25
- El-Zaher MA (2013) A Comparative study of the indoor radon level with the radon exhalation rate from soil in Alexandria city. *Radiat Prot Dosim* 154(4):490–496
- Faanu A, Darko EO, Ephraim JH (2011) Determination of natural radioactivity and hazard in soil and rock samples in a mining area in Ghana. *West African J App Eco* 19:77–92

- Gaware JJ, Sahoo BK, Sapra BK, Mayya YS (2011) Development of online radon and thoron monitoring systems for occupation and general environments. *BARC News Letter ISSN 0976-2108* (318): 45–51
- Gulan L, Milenkovic B, Stajic JM, Vuckovic B, Krstic D, Zeremski T, Ninkov J (2013) Correlation between radioactivity levels and heavy metal content in the soils of the North Kosovska Mitrovica environment. *Environ Sci. Processes Impacts* 15:1735–1742. <https://doi.org/10.1039/c3em00208j>
- Gusain GS, Rautela BS, Sahoo SK, Ishikawa T, Prasad G, Omori Y, Sorimachi A, Tokonami S, Ramola RC (2012) Distribution of terrestrial gamma radiation dose rate in the eastern coastal area of Odisha, India. *Radiat Prot Dosim* 152(1-3):42–25. <https://doi.org/10.1093/rpd/ncs148>
- Hassan NM, Ishikawa T, Hosoda M, Sorimachi A, Tokonami S, Fukushima M, Sahoo SK (2010) Assessment of the natural radioactivity using two techniques for the measurement of radionuclide concentration in building materials used in Japan. *J Radioanal Nucl Chem* 283:15–21. <https://doi.org/10.1007/s10967-009-0050-6>
- IAEA (2002). Radiation legacy of the 20th century: environmental restoration. International Atomic Energy Agency.
- Ielsch G, Ferry C, Tymen G, Robe MC (2002) Study of a predictive methodology for quantification and mapping of the radon-222 exhalation rate. *J Environ Radioact* 63:15–33. [https://doi.org/10.1016/S0265-931X\(01\)00133-3](https://doi.org/10.1016/S0265-931X(01)00133-3)
- Jadiyappa (2018) Radioisotope: applications, effects, and occupational protection. In book: principles and applications in nuclear engineering radiation effects, thermal hydraulics, radionuclide migration in the environment. Chapter 2 Intech Open, pp 19–47. <https://doi.org/10.5772/intechopen.79161>
- Kaul R, Umamaheshwar K, Chandrasekaran E, Deshmukh RD, Swarnkar BM (1993) Uranium mineralization in the Siwaliks of NW Himalayas, India. *J Geol Soc India* 41:243–258
- Kaur M, Kumar A, Mehra R, Mishra R (2017) Study of soil radon gas concentration and radon exhalation rate in the lower Himalayas of Jammu & Kashmir (India). *J Environ Biol* 31(2):453–458 ISSN 0973-6913 (Print), ISSN 0976-3384 (On Line)
- Kaur M, Kumar A, Mehra R, Mishra R (2018a) Human health risk assessment from exposure of heavy metals in soil samples of Jammu district of Jammu & Kashmir. *India Arabian J Geosciences*. <https://doi.org/10.1007/s12517-018-3746-5>
- Kaur M, Kumar A, Mehra R, Mishra R, Sharma N (2018b) Assessment of primordial and anthropogenic radionuclide contents in the soil samples of lower Himalayas of Jammu & Kashmir, India. *J Radioanal Nucl Chem* 317:1165–1174. <https://doi.org/10.1007/s10967-018-5988-9>
- Kaur M, Kumar A, Mehra R, Mishra R (2018c) Study of radon/thoron exhalation rate, soil-gas radon concentration, and assessment of indoor radon/thoron concentration in Siwalik Himalayas of Jammu & Kashmir. *Hum Ecol Risk Assess* 24(8):2275–2287. <https://doi.org/10.1080/10807039.2018.1443793>
- Kumar A, Kumar A, Singh Y, Singh S, Kumar V, Singh S (2009) Radioactivity measurements in the environ of the Udhampur Area, Jammu & Kashmir Himalayas, India. *Radiat Effects & Defects in Solids* 164(11):719–725. <https://doi.org/10.1080/10420150903092280>
- Mann HB, Whitney DR (1947) On a test of whether one of two random variable is stochastically larger than the other. *Ann Math Stat* 18:50–60. <https://doi.org/10.1214/aoms/1177730491>
- Mehta V, Singh SP, Chauhan RP, Muduar GS (2015) Study of indoor radon, thoron and their progeny concentration and radon exhalation rate in the environs of Mohali Punjab, Northern India. *Aero Air and Quality Res* 15:1380–1389. <https://doi.org/10.4209/aaqr.2014.08.0161>
- Menon SR, Sahoo BK, Balasundar S, Gaware JJ, Jose MT, Venkatraman B, Mayya YS (2015) A comparative study between the dynamic method and passive can technique of radon exhalation measurements from Samples. *Appl Radiat Isot* 99:172–178. <https://doi.org/10.1016/j.apradiso.2015.02.004>
- Mir FA, Rather SA (2015) Measurement of radioactive nuclides present in soil samples of district Ganderbal of Kashmir Province for radiation safety purposes. *J Radiat Res Appl Sci* 8:155–159. <https://doi.org/10.1016/j.jrras.2014.03.006>
- Mujahid SA, Hussain S, Ramzan M (2010) Measurement of radon exhalation rate and soil gas radon concentration in areas of southern Punjab, Pakistan. *Radiat Prot Dosim* 140(3):300–303. <https://doi.org/10.1093/rpd/ncq119>
- Nazaroff WW, Nero AV Jr (1988) *Indoor Air*. John Wiley and Sons Inc. (Ed.), Radon and its decay products in Indoor Air, 57–112. N Y ISBN-13: 978-0471628101 ISBN-10: 0471628107
- NCRP (1987). National Council on Radiation Protection and Measurements. Report No. 93, Ionizing radiation exposure of the population of the United States (1987).
- OECD (2009). Exposure to radiation from natural radioactivity in building materials nuclear energy agency.
- Prajith R, Rout RP, Kumbhar D, Mishra R, Sahoo BK, Sapra BK (2019) Measurement of radon (²²²Rn) and (²²⁰Rn) exhalations and their decay product concentrations at India stations in Antarctica. *Environ Earth Sci* 78(35). <https://doi.org/10.1007/s12665-018-8029-7>
- Rafique M, Rahman SU, Mehmood T, Rahman S, Matiullah RSU (2011) Radon exhalation rate from soil, sand, bricks and sedimentary samples collected from Azad Kashmir, Pakistan. *Russ Geol Geophys* 52(4):451–458. <https://doi.org/10.1016/j.rgg.2011.03.007>
- Raghu Y, Ravisankar R, Chandrasekaran A, Vijaygopal P, Venkatraman B (2016) Assessment of natural radioactivity and radiological hazards in brick samples used in Tiruvannamalai District, Tamilnadu, India, with a statistical approach. *Health Phys* 111(3):265–280
- Rahman SU, Faheem M, Anwar J, Ziafat M, Nasir T, Matiullah (2009) External dose assessment from the measured radioactivity in soil samples collected from the Islamabad capital territory, Pakistan. *J Radiol Prot* 29:499–505. <https://doi.org/10.1088/0952-4746/29/4/004>
- Rahman SU, Matiullah MF, Rafique M, Anwar J, Ziafat M, Jabbar A (2011) Measurement of naturally occurring/fallout radioactive elements and assessment of annual effective dose in soil samples collected from four districts of the Punjab Province, Pakistan. *J Radioanal Nucl Chem* 287:647–655. <https://doi.org/10.1007/s10967-010-0819-7>
- Ramola RC, Yadav M, Gusain GS (2014) Distribution of natural radionuclide along Main Central Thrust in Garhwal Himalaya. *J Radiat Res App* 7(4):614–619. <https://doi.org/10.1016/j.jrras.2014.10.002>
- Rani A, Mittal S, Mehra R, Ramola RC (2015) Assessment of natural radionuclides in the soil samples from Marwar region of Rajasthan, India. *Appl Radiat Isot* 101:122–126. <https://doi.org/10.1016/j.apradiso.2015.04.003>
- Rogers VC, Nielson KK (1991) Multiphase radon generation and transport in porous materials. *Health Phys* 60(6):807–815. <https://doi.org/10.1097/00004032-199106000-00006>
- Saad AF, Abdallah RM, Hussain NA (2013) Radon exhalation rate from Libya soil samples measured with the SSNTD technique. *Appl Radiat Isot* 72:163–168. <https://doi.org/10.1016/j.apradiso.2012.11.006>
- Sahoo BK, Nathwani D, Eappen KP, Ramachandran TV, Gaware JJ, Mayya YS (2007) Estimation of radon emanation factor in Indian building materials. *Radiat Meas* 42:1422–1425. <https://doi.org/10.1016/j.radmeas.2007.04.002>
- Sahoo BK, Mayya YS, Sapra BK, Gaware JJ, Banerjee KS, Kushwaha HS (2010) Radon exhalation studies in Indian uranium tailings pile. *Radiat Meas* 45:237–241. <https://doi.org/10.1016/j.radmeas.2010.01.008>
- Sarap NB, Janković MM, Todorović DJ, Nikolić JD, Kovačević MS (2014) Environmental radioactivity in southern Serbia at locations

- where depleted uranium was used. *Arh Hig Rada Toksikol* 65(2): 189–197. <https://doi.org/10.2478/10004-1254-65-2014-2427>
- Shapiro SS, Wilk MB (1965) An analysis of variance test for normality (complete samples). *Biometrika* 52(3/4):591–611 <http://www.jstor.org/stable/2333709>
- Sharma DK, Kumar A, Kumar M, Singh S (2003) Study of uranium, radium and radon exhalation rate in soil samples from some areas of Kangra district, Himachal Pradesh, India using Solid State Nuclear Track Detector. *Radiat Meas* 36:363–366. [https://doi.org/10.1016/S1350-4487\(03\)00152-5](https://doi.org/10.1016/S1350-4487(03)00152-5)
- Shiroma Y, Hosoda M, Ishikawa T, Sahoo SK, Tokonami S, Furukawa M (2015) Estimation of radon emanation coefficient for representative soils in Okinawa, Japan. *Radiat Prot Dosim* 167(1-3):147–150. <https://doi.org/10.1093/rpd/ncv233>
- Singh S, Sharma DK, Dhar S, Kumar A, Kumar A (2007) Uranium, radium and radon measurements in the environs of Nurpur area, Himachal Himalayas, India. *Environ Monit Assess* 128:301–309. <https://doi.org/10.1007/s10661-006-9313-7>
- Singh P, Singh P, Bajwa BS, Sahoo SK (2016) Radionuclide contents and their correlation with radon-thoron exhalation in soil samples from mineralized zone of Himachal Pradesh, India. *J Radioanal Nucl Chem.* <https://doi.org/10.1007/S10967-016-4975-2>
- Sun K, Guo Q, Zhuo W (2004) Feasibility for mapping radon exhalation rate from soil in China. *J Nucl Sci Technol* 41(1):86–90. <https://doi.org/10.1080/18811248.2004.9715462>
- Tabar E, Yakut H, Ku A (2016) Measurement of the radon exhalation rate and effective radium concentration in soil samples of southern Sakarya. *Turkey Indoor Built Environ.* <https://doi.org/10.1177/1420326X16672510>
- UNSCEAR (1988) Early effects in man of high doses of radiation. In: Sources and Effects of Ionising Radiation Report to the General Assembly with Annexes (Annex G) United Nations. York, New York
- UNSCEAR (1993). Source and effect of ionizing radiation. United Nation Scientific Committee on the effect of atomic radiation, United Nation, New York.
- UNSCEAR (2000a). Annex B: exposure from natural sources radiation. Sources and Effects of Ionising Radiation Report to the General Assembly with Annexes. United Nations, New York.
- UNSCEAR (2000b). Exposure and effects of the Chernobyl accident. UN, New York.
- UNSCEAR (2000c). Exposures from natural radiation sources. UN, New York.
- Zhuo W, Iida T, Furukawa M (2006) Modeling radon flux density from the earth's surface. *J Nucl Sci Technol* 43(4):479–482. <https://doi.org/10.1080/18811248.2006.9711127>